Testing the meson cloud model in inclusive meson production

F. Carvalho,* F. O. Durães,† F. S. Navarra,‡ and M. Nielsen§
Instituto de Física, Universidade de São Paulo, C.P. 66318, 05315-970 São Paulo, SP, Brazil
(Received 23 October 1998; revised manuscript received 11 June 1999; published 8 October 1999)

We have applied the meson cloud model (MCM) to calculate inclusive momentum spectra of pions and kaons produced in high energy proton-proton and proton-nucleus collisions. For the first time these data are used to constrain the cloud cutoff parameters. We show that it is possible to obtain a reasonable description of data, especially the large x_F ($x_F \geq 0.2$) part of the spectrum and at the same time describe (partially) the E866 data on $\bar{d}-\bar{u}$ and $\bar{d}/\bar{u}$. We also discuss the relative strength of the πN and $\pi\Delta$ vertices. We find out that the corresponding cutoff parameters should be both soft and should not differ by more than 200 MeV from each other. An additional source (other than the meson cloud) of sea antiquark asymmetry seems to be necessary to completely explain the data. A first extension of the MCM to proton nucleus collisions is discussed. [S0556-2821(99)08119-9]

PACS number(s): 14.20.Dh, 12.40.−y, 13.85.Qk

I. INTRODUCTION

Recent measurements [1,2] have established the asymmetry in the distributions of up and down quarks in the nucleon sea, a result which cannot be understood in terms of perturbative QCD. The presence of pions in the nucleon can naturally account for the excess of $\bar{d}$ over $\bar{u}$. The role of mesons in deep inelastic scattering (DIS) was investigated by Thomas [3]. He suggested that some fraction of the nucleon's antiquark sea distribution may be associated with the pion cloud of the nucleon. Several works developed this idea and gave origin to the meson cloud model (MCM) [4–6]. They are all based on the notion that the physical proton (p) may be expanded in a sum of virtual meson-baryon (MB) states. The probabilities of these states are not known *a priori*. They are commonly related to the probability of the splitting $p \rightarrow MB$, which, in turn, is calculated with a simple Feynman diagram of meson emission. In these calculations the assumption is made that the proton is already an extended object and a form factor is assigned to the meson emission vertex. This form factor contains a cutoff parameter which must be adjusted by fitting experimental data. In some works it is adjusted to correctly reproduce the Gottfried sum rule (GSR) violation. The most consistent procedure, however, is to fix the cutoff by simultaneously analyzing data on hadronic collisions and parton distribution functions. This is the attitude adopted, for example, in [7]. The cutoff choices vary over a wide range according to the experimental source used in the determination procedure. In Ref. [8] a detailed discussion of the subject is presented.

In a very recent analysis of the E866 data [2], the authors used the MCM to fit the $\bar{d}(x)-\bar{u}(x)$ as a function of x. The dominant intermediate MB states are πN and $\pi\Delta$. The conclusion was that the cutoff associated with both states must be soft and also $\Lambda_{\pi N} \geq \Lambda_{\pi\Delta}$. In particular, with dipole form factor $\Lambda_{\pi N}=1.0$ GeV and $\Lambda_{\pi\Delta}=0.8$ GeV. A similar conclusion was reached in [8]. With such choices it was possible to find ''nearly exact accord'' with experiment. This finding on one hand increases the confidence in the virtual meson-baryon picture but on the other hand imposes constraints on the MCM description of other high energy collision data. In many previous studies $\Lambda_{\pi N}$ and $\Lambda_{\pi\Delta}$ were assumed to be roughly equal [7,9]. Shortly after the E866 analysis, Melnitchouk, Speth, and Thomas [10] presented a new calculation of the $\bar{d}-\bar{u}$ asymmetry in the framework of the MCM, including πN and $\pi\Delta$ states and also Pauli exclusion principle effects. Their conclusion was that data can be reproduced with a dipole form factor if $\Lambda_{\pi N}=1.0$ GeV and $\Lambda_{\pi\Delta}=1.3$ GeV.

In this work we address inclusive meson production at high energy proton-proton and proton-nucleus collisions. We concentrate on low p_T ($p_T \leq 0.3$ GeV) and large x_F ($x_F \geq 0.2$) where nonperturbative effects are dominant and the meson cloud is most relevant. More specifically we address the x_F distributions of π^+ and K^+ produced in pp and pA collisions at $p_{\rm lab} \simeq 100$ GeV/c. We present simultaneously a fit of the meson inclusive spectra and the analysis of the GSR including the recently measured $\bar{d}(x)-\bar{u}(x)$ distribution. Our purpose is to make a new test of the MCM and at the same time check the cutoff choices made in Refs. [2] and [10].

II. MESON SPECTRA IN THE MCM

Assuming that in proton-proton collisions the proton behaves like a meson (M)-baryon (B) state, the possible reaction mechanisms for meson production at large x_F and small p_T are illustrated in Fig. 1. In Fig. 1(a) the baryon just ''flies through,'' whereas the corresponding meson interacts inelastically producing a π^+ or a K^+ in the final state. In Fig. 1(b) the meson just ''flies through,'' whereas the corresponding baryon interacts inelastically producing a π^+ or a K^+ in the final state. In Fig. 1(c) the meson in the cloud is already a π^+ or a K^+ which escapes. We shall refer to the first two

*Email address: babi@if.usp.br
†Email address: fduraes@if.usp.br
‡Email address: navarra@if.usp.br
§Email address: mnielsen@if.usp.br

 ©1999 The American Physical Society

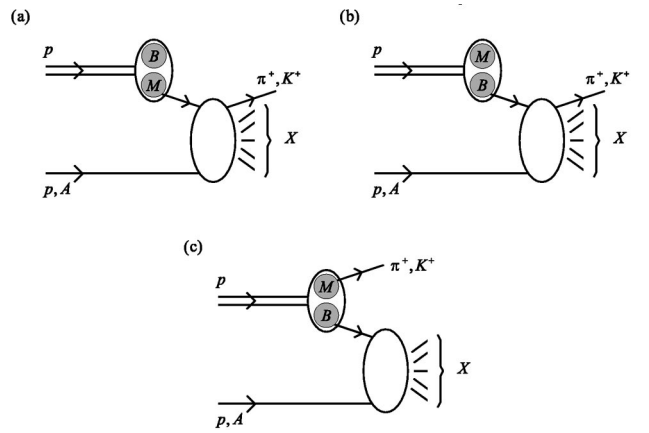

FIG. 1. pp or pA collision in which the projectile is in a $|MB\rangle$ state. (a) ''Indirect'' K^+ or π^+ production: the meson M from the cloud undergoes the reaction $Mp(A)\rightarrow\pi^+(K^+)X$. (b) ''Indirect'' K^+ or π^+ production: the baryon from the cloud undergoes the reaction $Bp(A)\rightarrow\pi^+(K^+)X$. (c) ''Direct'' K^+ or π^+ production: the cloud meson π^+ (K^+) escapes from the cloud as a spectator.

processes as ''indirect production'' and to the last one as ''direct production.'' The first two are calculated with convolution formulas whereas the last one is given basically by the meson momentum distribution in the cloud initial $|MB\rangle$ state. Direct production has been widely used in the context of the MCM and applied to study n, Δ^{++}, and π^0 production [7,11,12]. Indirect meson production has been considered previously in a simplified approach [13].

In Ref. [7] a process analogous to Fig. 1(c), in which the baryon escapes was used to determine various cutoff parameters. The authors found values around 1 GeV for all of them. However the agreement between theory and experiment was poor. This suggests that the no rescattering assumption is not appropriate. In [12] the same type of process was considered but rescattering of the baryon with the target was included and absorptive corrections were calculated. This results in a reduction of about 40% of the cross section at almost all values of the baryon fractional momentum (z) except at $z\simeq 1$ where absorptive corrections are not important. The indirect mechanism has not been applied to baryon production because the subprocess $Bp\rightarrow BX$ is not experimentally well known. On the other hand we can study inclusive meson production with Fig. 1(a) since data on $Mp\rightarrow MX$ are available.

As stated above, in the MCM the projectile proton is regarded as being a sum of virtual meson-baryon pairs and a proton-proton reaction can thus be viewed as reaction between the ''constituent'' mesons and baryons of one proton with the other proton.

We shall decompose the proton in the following possible Fock states:

$$|p\rangle = Z[|p_0\rangle + |p_0\pi^0\rangle + |n\pi^+\rangle + |\Delta^0\pi^+\rangle + |\Delta^+\pi^0\rangle + |\Delta^{++}\pi^-\rangle + |\Lambda K^+\rangle + |\Sigma^0 K^+\rangle + |\Sigma^{0*}K^+\rangle + |\Sigma^+ K^0\rangle + |\Sigma^{+*}K^0\rangle] \quad (1)$$

where $|p_0\rangle$ is the bare proton. We consider only light mesons. In [7] the state $|N\rho\rangle$ was also included but was found to be relevant only for production of large p_T particles. Since we will be restricted to low p_T production we shall neglect the havier mesons.

The relative normalization of these states is in principle fixed once the cloud parameters are fixed. Z is a normalization constant.

In the $|MB\rangle$ state the meson and baryon have fractional momentum y_M and y_B with distributions called $f_{M/MB}(y_M)$ and $f_{B/MB}(y_B)$, respectively. Of course $y_M+y_B=1$ and these distributions are related by

$$f_{M/MB}(z)=f_{B/MB}(1-z). \quad (2)$$

The ''splitting function'' $f_{M/MB}(y)$ represents the probability density to find a meson with momentum fraction y of the nucleon and is usually given by

$$f_{M/MB}(y)=\frac{g^2_{MBp}}{16\pi^2}y\int_{-\infty}^{t_{max}}dt\frac{[-t+(M_B-M_p)^2]}{[t-m_M^2]^2}F^2_{MBp}(t), \quad (3)$$

for baryons B belonging to the octet and

$$f_{M/MB}(y)=\frac{g^2_{MBp}}{16\pi^2}y\int_{-\infty}^{t_{max}}dt \times\frac{[(M_B+M_p)^2-t]^2[(M_p-M_B)^2-t]}{12M_B^2M_p^2[t-m_M^2]^2}F^2_{MBp}(t) \quad (4)$$

for baryons belonging to the decuplet. In the above equations t and m_M are the four momentum square and the mass of the meson in the cloud state, t_{max} is the maximum t given by

$$t_{max}=M_B^2y-\frac{M_p^2y}{1-y}, \quad (5)$$

M_B (M_p) is the mass of the baryon B (p). Since the function $f_{M/MB}(y)$ has the interpretation of ''flux'' of mesons M inside the proton, the corresponding integral

$$n_{M/MB}=\int_0^1 dy f_{M/MB}(y) \quad (6)$$

can be interpreted as the ''number of mesons'' in the proton or ''number of mesons in the air.'' In many works the magnitude of the multiplicities $n_{M/MB}$ has been considered a measure of the validity of MCM in the standard formulation with MB states. If these multiplicities turn out to be large $(\simeq 1)$ then there is no justification for employing a one-meson truncation of the Fock expansion. The model has no longer convergence. This may happen for large cutoff values.

The invariant cross section for production of positively charged mesons M^+ $(\pi^+$ or $K^+)$ is given by

$$E\frac{d^3\sigma^{pp\to M^+X}}{dp^3}=\frac{x_F}{\pi}\frac{d\sigma^{pp\to M^+X}}{dx_F dp_T^2}=\Phi_M+\Phi_B+\Phi_D \quad (7)$$

where

$$\Phi_M=\sum_{MB}\int_{x_F}^1\frac{dy}{y}f_{M/MB}(y)\frac{x_F}{\pi y}\frac{d\sigma^{M+p\to M^+X}}{d(x_F/y)dp_T^2}(x_F/y) \quad (8)$$

and

$$\Phi_B=\sum_{MB}\int_{x_F}^1\frac{dy}{y}f_{B/MB}(y)\frac{x_F}{\pi y}\frac{d\sigma^{B+p\to M^+X}}{d(x_F/y)dp_T^2}(x_F/y). \quad (9)$$

Φ_M and Φ_B refer respectively to the indirect meson and baryon initiated reactions and x_F and p_T are respectively the fractional longitudinal momentum and transverse momentum of the outgoing meson. The sum is over all the cloud states in Eq. (1).

Φ_D represents the direct process depicted in Fig. 1(c) and is given by

$$\Phi_D=\sum_{MB}f_{M/MB}(x_F,p_T^2)\sigma^{Bp}(s_X)K_{abs}, \quad (10)$$

where $f_{M/MB}(x_F,p_T^2)$ is given by Eqs. (3) and (4), not integrated over t and with the replacement $t=-p_T^2/(1-x_F)-x_F^2M_B^2/(1-x_F)$. The quantity $\sigma^{Bp}(s_X)$ is the baryon-proton cross section at center-of-mass system energy $\sqrt{s_X}$ and K_{abs} is an absorption factor. This cross section is energy (s_X) dependent but in the energy range considered here its variation is very small and therefore we take it as a constant $\sigma^{Bp}=38$ mb. The K factor was used in Refs. [12,14] to account for rescattering of the escaping cloud element (in that case a baryon and here a meson) against the proton target. It varies in the range $0\leqslant K_{abs}\leqslant 1$ and expresses the efficiency of the direct process. Of course this is a model dependent quantity. As stated above, the modest agreement of direct production calculations with data obtained in several works and the improvement obtained in [12,14] (with the inclusion of absorption effects) strongly suggest that this factor is important and we shall keep it.

Once the '' splitting functions'' equations (3) and (4) are known we can calculate the part of the antiquark distribution in the proton coming from the pion cloud with the convolution

$$\overline{q}(x)_f=\int_x^1\frac{dy}{y}f_{M/MB}(y)\overline{q}_f^{\pi}\left(\frac{x}{y}\right), \quad (11)$$

where $\overline{q}_f^{\pi}(z)$ is the flavor f valence antiquark distribution in the pion. With the above formula we can compute the $\overline{d}$ and $\overline{u}$ distributions, their difference, $D=\overline{d}(x)-\overline{u}(x)$, and calculate the Gottfried integral:

$$S_G=\frac{1}{3}-\frac{2}{3}\int_0^1[\overline{d}(x)-\overline{u}(x)]dx. \quad (12)$$

TABLE I. Subprocesses contributing to inclusive meson production ($M^+=\pi^+$ or K^+).

$Mp\to M^+X$	$Bp\to M^+X$	$Bp\to M^+X$
$\pi^+p\to M^+X$	$np\to M^+X$	$\Lambda p\to M^+X$
$\pi^0p\to M^+X$	$p_0p\to M^+X$	$\Sigma^0p\to M^+X$
$\pi^-p\to M^+X$	$\Delta^0p\to M^+X$	$\Sigma^{0*}p\to M^+X$
$K^+p\to M^+X$	$\Delta^+p\to M^+X$	$\Sigma^+p\to M^+X$
$K^0p\to M^+X$	$\Delta^{++}p\to M^+X$	$\Sigma^{+*}p\to M^+X$

III. INPUTS FOR THE CALCULATION

A. ''Elementary cross sections''

The invariant cross sections for the reactions $Mp\to M^+X$ and $Bp\to M^+X$, appearing in the convolutions (8) and (9) are listed in Table I. Those in the first column can be taken directly from experimental data [15,16]. The unmeasured $\pi^0p\to M^+X$ process was approximated by the average between $\pi^+p\to M^+X$ and $\pi^-p\to M^+X$. The same procedure was used for the process $K^0p\to M^+X$.

In making use of experimental cross sections we are treating the virtual mesons in the cloud as real particles. In our case this can be justified because the observed mesons both on the left-hand side of Eq. (7) and on the right-hand side of Eq. (8) and of Eq. (9) have very small tranverse momentum. Consequently the involved cloud particles must also have small tranverse momentum, being therefore not far from the mass shell.

The reactions in the second and third columns of Table I are not measured. We expect them all to be of the same order of magnitude (additive quark model approximation). We therefore approximate all these cross sections by an ''average cross section.'' In the case of π^+ and K^+ production we shall assume respectively that

$$\frac{x_F d\sigma^{Bp\to\pi^+X}}{\pi dx_F dp_T^2}\simeq\frac{x_F d\sigma^{pp\to\pi^+X}}{\pi dx_F dp_T^2},$$

$$\frac{x_F d\sigma^{Bp\to K^+X}}{\pi dx_F dp_T^2}\simeq\frac{x_F d\sigma^{pp\to K^+X}}{\pi dx_F dp_T^2}. \quad (13)$$

This implies that all baryons are equally efficient as the proton to produce π^+ or K^+ in collisions with a target proton. The absorption factor appearing in Eq. (10) is chosen to be $K_{abs}=0.4$ for pion production and $K_{abs}=0.8$ for kaon production. These values are within the range of theoretical estimates presented in [14].

B. Coupling constants

The coupling constants are either measured, inferred from isospin symmetry or estimated with, for example, QCD sum rules. We will take them from other works [8,9,17,7] and keep them fixed. They are given in Table II.

TABLE II. Coupling constants.

$g_{p\pi^+n}$	$\sqrt{2}g_{p\pi^0p}=\sqrt{2}(-3.795\sqrt{4\pi})$
$g_{p\pi^0p}$	$-3.795\sqrt{4\pi}$
$g_{p\pi^+\Delta^0}$	$\frac{1}{\sqrt{6}}g_{p\pi\Delta}=\frac{1}{\sqrt{6}}28.6$
$g_{p\pi^0\Delta^+}$	$\sqrt{2}g_{p\pi^+\Delta^0}=\frac{1}{\sqrt{3}}28.6$
$g_{p\pi^-\Delta^{++}}$	$\sqrt{3}g_{p\pi^+\Delta^0}=\frac{1}{\sqrt{2}}28.6$
$g_{K^+p\Lambda}$	$-3.944\sqrt{4\pi}$
$g_{K^+p\Sigma^{*0}}$	$\frac{1}{\sqrt{3}}g_{Kp\Sigma*}=\frac{1}{\sqrt{3}}\frac{1}{2}g_{p\pi\Delta}=\frac{1}{\sqrt{3}}\frac{1}{2}28.6$
$g_{K^+p\Sigma^0}$	$\frac{1}{\sqrt{3}}g_{Kp\Sigma}=\frac{1}{\sqrt{3}}\frac{\sqrt{3}}{5}g_{p\pi^0p}=2.69$
$g_{K^0p\Sigma^{*+}}$	$\sqrt{2}g_{K^+p\Sigma^0*}=\sqrt{2}\frac{1}{\sqrt{3}}\frac{1}{2}28.6$
$g_{K^0p\Sigma^+}$	$\sqrt{2}g_{K^+p\Sigma^0}=\sqrt{2}\ 2.69$

C. Cutoff parameters

In the calculations we need the baryon-meson-baryon form factors appearing in the splitting functions. Following a phenomenological approach, we use the dipole form

$$F_{MBp}(t)=\left(\frac{\Lambda_{MBp}^2-m_M^2}{\Lambda_{MBp}^2-t}\right)^2. \tag{14}$$

In the above formula Λ_{MBp} is the form factor cutoff parameter.

In [8] an extensive discussion concerning the appropriate value of the cutoff has been made, using exponential form factors. The conclusion of the authors was that, for exponential form factors, $\Lambda_{\pi NN}^e\simeq 1000$ MeV, $\Lambda_{\pi N\Delta}^e\simeq 800$ MeV, and $\Lambda_{KNY}^e\simeq 1200$ MeV. They find out that allowing the πNN and $\pi N\Delta$ vertices to be different improves the quality of their fits. On the strange sector, on the other hand, they use a harder and universal cutoff. In Ref. [7] the MCM was used to study baryon (n, Λ, and Δ^{++}) spectra in pp collisions and the resulting fits strongly suggest a universal cutoff $\Lambda^e\simeq 1000$ MeV. The exponential form factor is, of course, not the only possible choice. One might use a monopole or dipole form as well. Differences between the various forms are not particularly important and, besides, as it was pointed out by Kumano [18] it is possible to ''translate'' one form factor with its cutoff to another form factor with a correspondingly different cutoff, the overall results being approximately equivalent. The approximate relation between the exponential (e), dipole (d), and monopole (m) cutoffs is given by $\Lambda^m\simeq 0.62\Lambda^d\simeq 0.78\Lambda^e$. As pointed out in [8], in dealing with decuplet splitting functions monopole form factors lead to divergencies. With an exponential form factor one avoids this problem but the calculations can only be done numerically. Using the dipole form factor we can perform the integrations (3) and (4) analytically. Because of this advantage we choose the dipole form.

Once translated to the monopole form the cutoff values quoted above give values around 800 MeV which are still significantly smaller than old analyses performed with the Bonn potential [17] or the Nijmegen [19] potential which favor a harder cutoff ($\Lambda^m\simeq 1000$ MeV) but are close to values obtained in more recent analyses performed by the same group [20].

In view of all the works done so far on this subject, we may conclude that these cutoff parameters must be soft. The next question which is now under debate is: which cutoff is larger, $\Lambda_{\pi NN}$ or $\Lambda_{\pi N\Delta}$? As pointed out in the introduction, the E866 analysis [2] favors $\Lambda_{\pi NN}\geqslant\Lambda_{\pi N\Delta}$ whereas Melnitchouk, Speth, and Thomas [10] suggest that $\Lambda_{\pi NN}\leqslant\Lambda_{\pi N\Delta}$.

Inspired on these two works we shall test the following choices for the dipole cutoff parameters:

$$(I)\ \ \Lambda_{oct}=0.96\ \text{GeV},\quad \Lambda_{dec}=0.77\ \text{GeV},$$

$$(II)\ \ \Lambda_{oct}=0.87\ \text{GeV},\quad \Lambda_{dec}=1.0\ \text{GeV}. \tag{15}$$

Λ_{oct} and Λ_{dec} are the cutoff parameters for all the octet and decuplet vertices, respectively. As it will be seen, these choices are in reasonable agreement with experimentally measured meson x_F spectra.

IV. RESULTS AND DISCUSSION

Before presenting a comparison with experimental data we show in Fig. 2 the behavior of the splitting functions $f_{M/MB}$ and $f_{B/MB}$ with respect to cutoff variations. Solid and dashed lines represent respectively the octet equation (3) and decuplet equation (4) MB states. The two upper (lower) boxes show functions calculated with soft (hard) cutoff parameters. The upper and lower boxes on the left (right) show functions with octet cutoff parameters harder (softer) than the decuplet ones. The values, chosen for the purpose of illustration, are: $\Lambda_{oct}=1.0$ GeV and $\Lambda_{dec}=0.80$ GeV [Fig. 2(c)]; $\Lambda_{oct}=0.80$ GeV and $\Lambda_{dec}=1.0$ GeV [Fig. 2(b)]; $\Lambda_{oct}=2.0$ GeV and $\Lambda_{dec}=1.6$ GeV (Fig. 2(c)]; $\Lambda_{oct}=1.6$ GeV and $\Lambda_{dec}=2.0$ GeV [Fig. 2(d)]. We consider the momentum (y) distributions of π^+ in the states π^+n and $\pi^+\Delta^0$ and also the baryon momentum ($y_B=1-y$) distribution in these states. Because of Eq. (2) all these figures are symmetric and the meson momentum distributions (always on the left part of each box) are the ''mirror'' pictures of the corresponding baryon momentum distributions (always on the right part of each box). The comparison between the upper panels with the lower ones shows that at soft cutoff's there is a more distinct separation between baryons and mesons, the former peaking at higher values of y and the latter at smaller y's. At harder cutoff's all the curves tend to become identical and centered at $y=0.5$. The decuplet functions lie always below the octet functions, except if $\Lambda_{dec}\gg\Lambda_{oct}$, which is unrealistic. In Fig. 2(d) we can see that

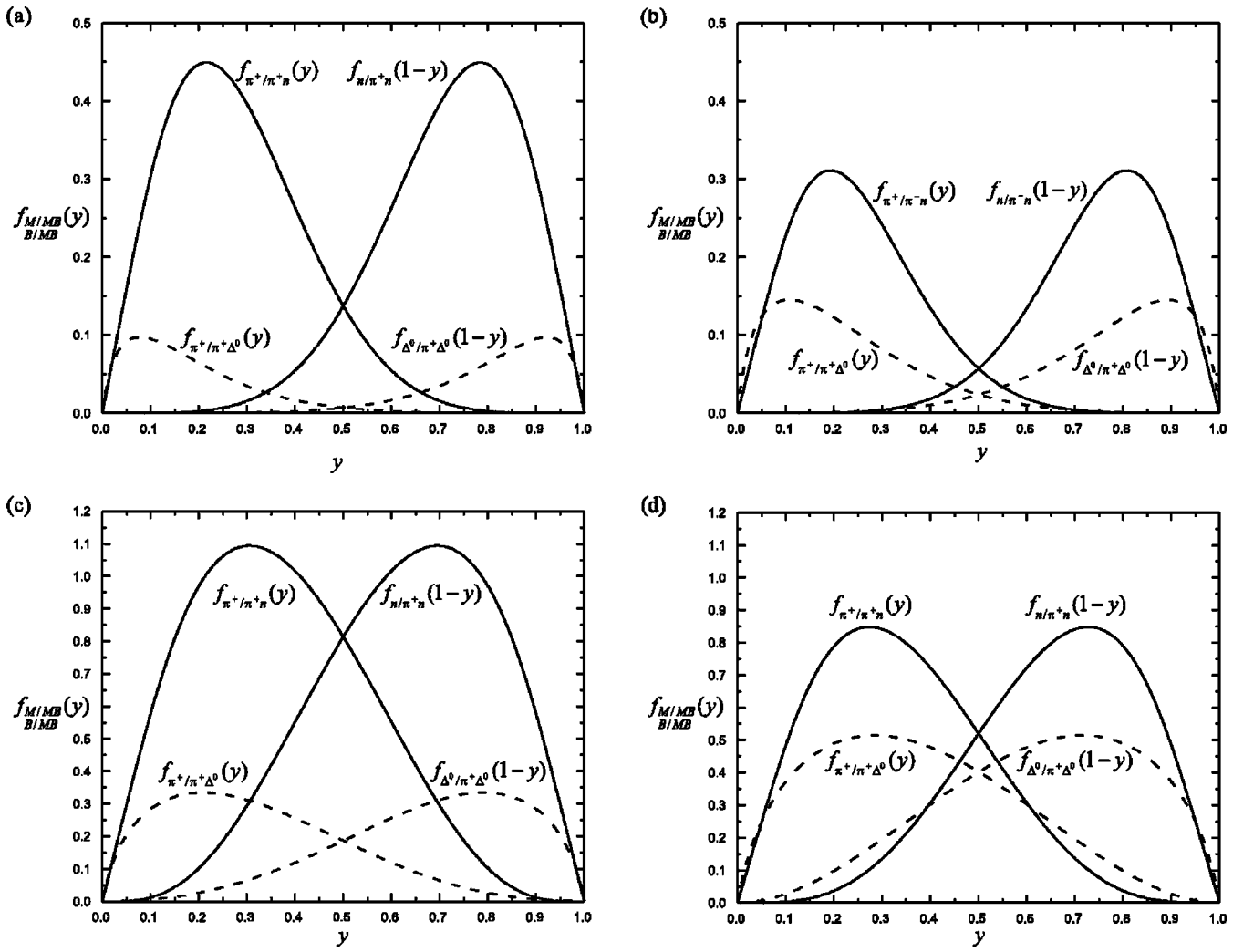

FIG. 2. Illustration of the octet (decuplet) splitting functions $f_{M/MB}$ and $f_{B/MB}$ in solid (dashed) lines for the following cutoff choices: (a) $\Lambda_{oct}=1.0$ GeV and $\Lambda_{dec}=0.80$ GeV; (b) $\Lambda_{oct}=0.80$ GeV and $\Lambda_{dec}=1.0$ GeV; (c) $\Lambda_{oct}=2.0$ GeV and $\Lambda_{dec}=1.6$ GeV; (d) $\Lambda_{oct}=1.6$ GeV and $\Lambda_{dec}=2.0$ GeV.

$f_{\pi^+/\pi^+\Delta^0}(y)$ lies above f_{π^+/π^+n} for $y\geqslant 0.6$. This feature was found in [10] to be very important in the study of sea antiquark asymmetry.

Using, as input, the splitting functions shown in Figs. 2(a), 2(b), 2(c), and 2(d), Eq. (7) for $M^+=\pi^+$ we obtain the pion spectra shown in Figs. 3(a), 3(b), 3(c), and 3(d), respectively. They are decomposed in meson initiated (M), Eq. (8) (dot-dashed lines), baryon initiated (B), Eq. (9) (dashed lines), direct (D), Eq. (10) (dotted lines), and the total sum (T). We see that the direct process dominates pion production up to $x_F\simeq 0.7$. In the two lower figures (harder cutoff parameters) they are so important for all x_F that one can neglect the M and B contributions. For soft cutoff choices the B component becomes important too and even dominant at $x_F\geqslant 0.8$ [shaded area in Figs. 3(a) and 3(b)]. Comparing the two shaded areas, we observe that with $\Lambda_{\pi NN}\leqslant\Lambda_{\pi N\Delta}$ (on the right) the B component starts earlier to dominate the pion x_F spectrum. This component is the harder and flatter one and is essential to obtain a good description of data at large x_F. The direct contribution alone would fall too fast and underestimate data. Neglecting the direct contribution leads to a good fit only with the M and B components but at the expense of unrealist large (dipole) cutoff choices: $\Lambda_{oct}=1.13$ GeV and $\Lambda_{dec}=1.8$ GeV. Only with these large numbers we recover the normalization of the experimental spectrum. Neglecting also the B component leads to a good fit with the M component alone and a cutoff $\Lambda_{oct}=2.1$ GeV. In short, it is clear that we need all three components to describe data, the first one (D) to get the proper normalization and the last two (B and M) to get the correct shape of the meson spectra. In this way we get also reasonable pion (and also kaon) multiplicities. For both cases (I and II) we obtain $n_\pi\simeq 0.17$, which is small enough to justify the use of the one-meson truncation of the Fock decomposition.

In Figs. 4(a) and 4(b) we present our pion and kaon spectra compared with experimental data, circles from Ref. [15] and triangles from Ref. [16]. In these figures we include all three components and plot Eq. (7) with the cutoff choices I (solid line) and II (dashed line). As it can be seen, the overall agreement with data is good over a large range on x_F. We have checked that significant deviations from these choices lead to large disagreement between our spectra and data. As

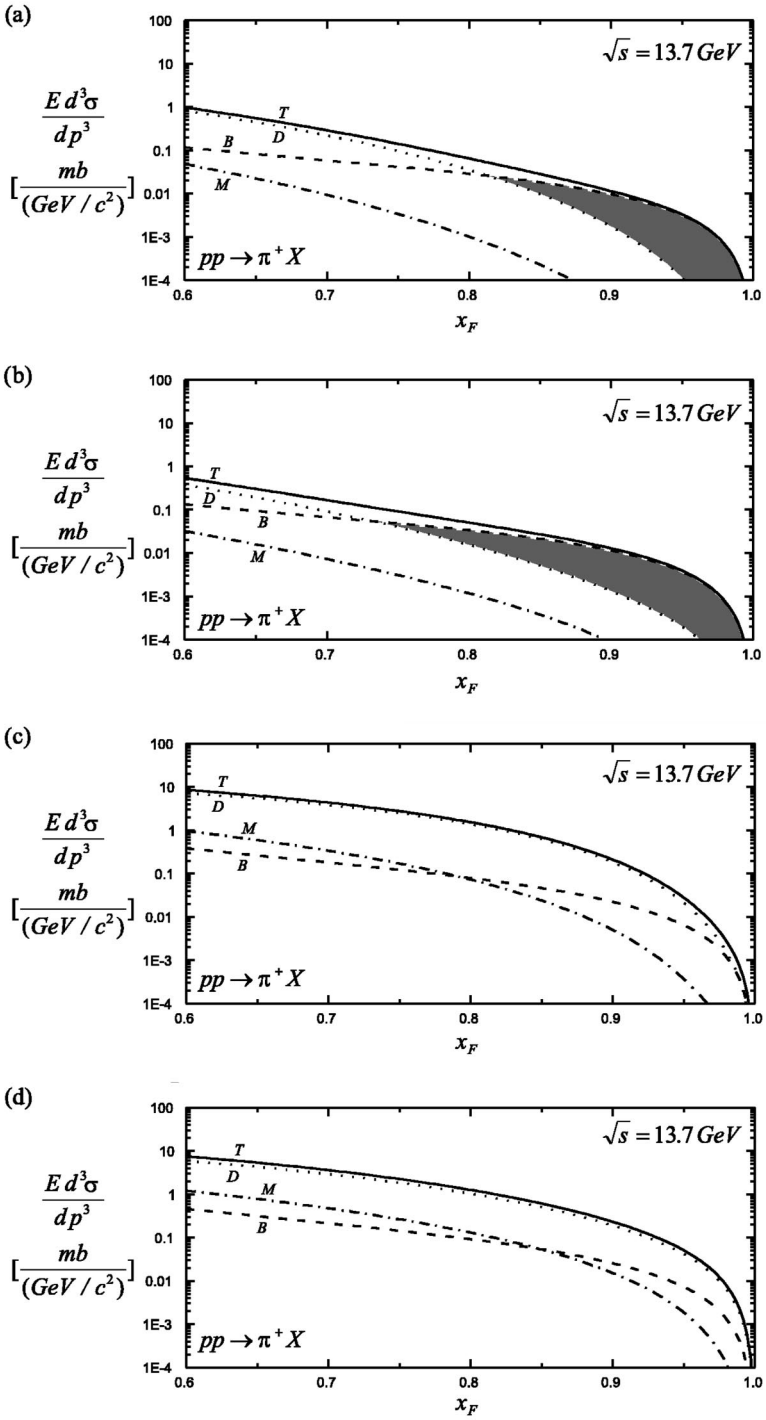

FIG. 3. Total (T) inclusive pion spectra in pA collisions calculated with Eq. (7) and the direct (D), meson initiated (M), and baryon initiated (B), given respectively by Eqs. (10), (8), and (9). (a), (b), (c), and (d) correspond to the cutoff choices made in Fig. 2.

an example we show in Fig. 4 with dotted lines the spectra corresponding to the the choice $\Lambda_{oct}=1.0$ GeV and $\Lambda_{dec}=1.3$ GeV discussed in [10]. As it can be seen they are already somewhat far from data points, especially in the case of the kaon spectrum. From this figure we may conclude that the MCM can give an accurate description of data with soft ($\Lambda \leqslant 1.0$ GeV) cutoff parameters. Choosing $\Lambda_{oct} \geqslant \Lambda_{dec}$ or $\Lambda_{oct} \leqslant \Lambda_{dec}$ does not make much difference as long as both cutoff's differ only by $\simeq 200$ MeV.

In Figs. 5(a) and 5(b) we show the difference $\overline{d}-\overline{u}$ and ratio $\overline{d}/\overline{u}$, respectively. The quark distribution functions were calculated with the convolution formula (11). The points represent the E866 data. Solid and dashed lines represent the parameter choices I and II, respectively. As expected our solid lines are very close to the ones presented by the E866 analysis in [2]. Using a larger cutoff for the $\pi N\Delta$ vertices leads to the dashed curves. As pointed out in [10] this choice leads to a reduction in the antiquark asymmetry, leaving room for additional sources of asymmetry, such as the Pauli exclusion principle.

The value of the Gottfried integral given by Eq. (12) is $S_G=0.261$ (case I) and $S_G=0.314$ (case II). The value re-

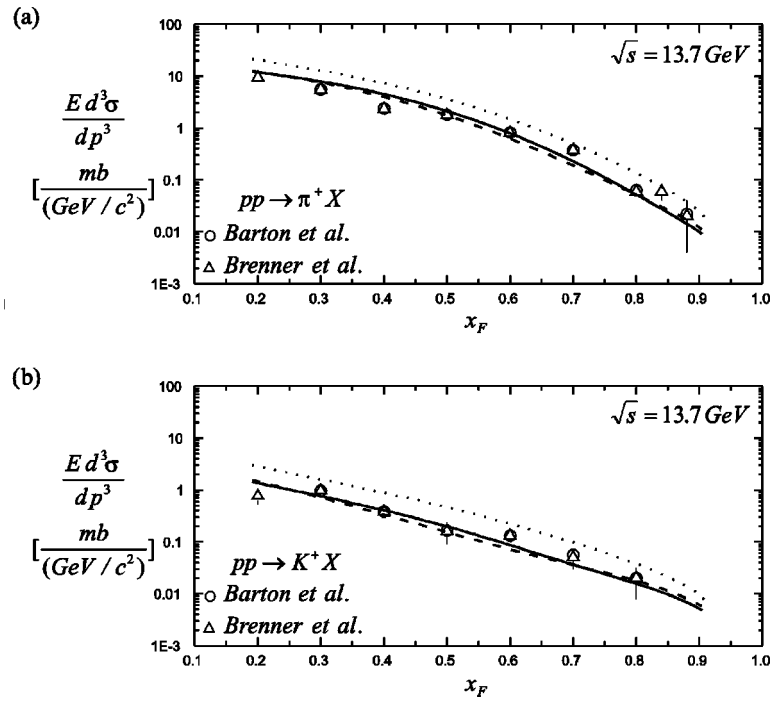

FIG. 4. (a) Inclusive pion spectra calculated with Eq. (7). Data are from [15,16]. Solid, dashed, and dotted lines correspond to the cutoff choices I, II, and $\Lambda_{\pi N}=1.0$ GeV, $\Lambda_{\pi\Delta}=1.3$ GeV, respectively; (b) the same as (a) for kaon spectra.

ported by the New Muon Collaboration (NMC) is 0.235 ± 0.026. Taken together, Figs. 4 and 5 and the integral S_G, it seems that choice I is better everywhere but fails badly in the $\overline{d}/\overline{u}$ ratio. Choice II, on the other hand, is never far from data points but gives a too large value for S_G. We thus conclude that a better global description of data can be obtained with Λ_{oct} moderately smaller than Λ_{dec} and that some additional source of asymmetry, other than the meson cloud, is required.

Another interesting test for the MCM is inclusive meson production in proton nucleus collisions. In principle we can use the same formulas Eqs. (7), (8), (9), and (10), replacing the cross sections $\sigma^{M(B)+p\to M^+X}$ by $\sigma^{M(B)+A\to M^+X}$ and keeping exactly the same splitting functions. However most of the $M(B)+A\to M^+X$ cross sections are not measured. As a first test we shall assume, following the experimental analysis described in Refs. [15,16], that

$$E\frac{d^3\sigma^{pA\to M^+X}}{dp^3} \simeq \text{const}\quad A^\alpha E\frac{d^3\sigma^{pp\to M^+X}}{dp^3}, \tag{16}$$

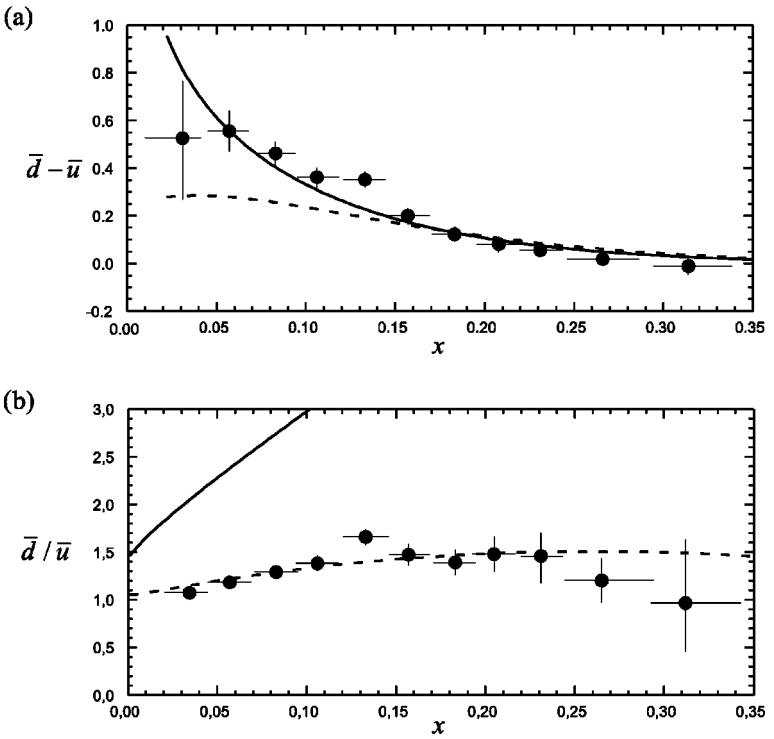

FIG. 5. (a) $\overline{d}-\overline{u}$ calculated with Eq. (11) with cutoff choices I (solid line) and II (dashed line) compared with E866 data; (b) the same as (a) for the ratio $\overline{d}/\overline{u}$.

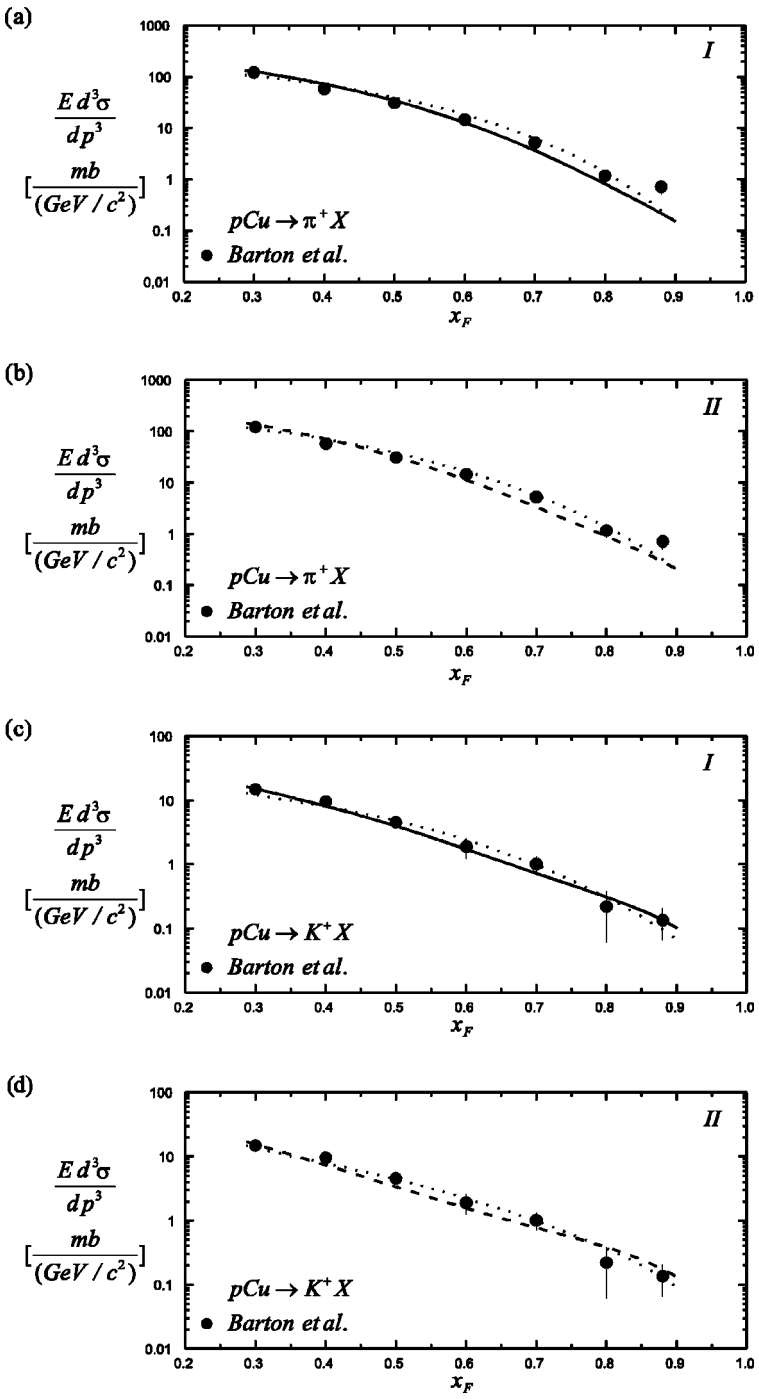

FIG. 6. Inclusive meson spectra in proton nucleus collisions calculated with Eq. (16) using cutoff choices I (solid lines) and II (dashed lines). Dotted lines show the curves obtained taking medium effects into account. Data are from [15,16]. (a) Pion spectrum with choice I; (b) pion spectrum with choice II; (c) same as (a) for kaons; (d) same as (b) for kaons.

where the constants are chosen to reproduce the normalization of data points. Usually α is a very slowly varying function of x_F. We take it constant ($\alpha=0.72$). The main goal of this exploratory study is only to test the shape of the spectra obtained with the MCM. In the above expression the pp cross sections are exactly the same as before. In Fig. 6 we show the spectra obtained with Eq. (16) for pions [Fig. 6(a) and 6(b)] and for kaons [Fig. 6(c) and 6(d)]. The cutoff choice I (II) is depicted with solid (dashed) line. Since the $|MB\rangle$ state will interact inside the nucleus it may be affected by medium effects. The simplest way to incorporate these effects is by changing the baryon masses according to $M_B \to M_B^* \simeq 0.8 M_B$. With this modification the meson splitting functions will increase in normalization and will peak at larger values of y_M. Because of this the final meson spectra will also peak at larger values of x_F. The inclusion of medium effects (curves in dotted lines in Fig. 6) improves the agreement between the MCM and data.

V. CONCLUSIONS

This work was motivated by the recent revival of the meson cloud picture of the nucleon. We performed a comparison between inclusive meson spectra predicted by the MCM and experimental data. Instead of using only the ''direct process,'' as done in Refs. [12,7] we have included the ''indirect

process,'' in which the final cross section is a convolution of the MCM ''splitting functions'' with the ''elementary'' meson-nucleon and baryon-nucleon cross sections, in an analogous way as done in the QCD parton model calculations. In this way we can test the universal splitting functions and determine the cutoff parameters. This determination is done by simultaneouly analyzing mesonic spectra, difference and ratio of antiquark distributions and the Gottfried sum rule.

The first conclusion of this work is that the MCM describes reasonably well the production of pions and kaons in pp high energy collisions. Even the intermediate x_F region $(0.2 \leqslant x_F \leqslant 0.6)$ is reproduced.

Concerning the relative strength of the nucleon and delta vertices, we find that the MCM can give a good description of data with soft ($\Lambda \leqslant 1.0$ GeV) cutoff parameters. Choosing $\Lambda_{oct} \geqslant \Lambda_{dec}$ or $\Lambda_{oct} \leqslant \Lambda_{dec}$ does not make much difference as long as both cutoffs differ only by $\simeq 200$ MeV. The latter choice seems to be more appropriate, especially if one introduces additional sources of sea asymmetry.

ACKNOWLEDGMENTS

This work has been supported by CNPq and FAPESP under contract number 98/2249-4. We are indebted to Y. Hama, F.M. Steffens, A.W. Thomas, and G. Krein for fruitful discussions.

[1] E866/NuSea Collaboration, E.A. Hawker *et al.,* Phys. Rev. Lett. **80**, 3715 (1998).
[2] E866/NuSea Collaboration, J.C. Peng *et al.*, Phys. Rev. D **58**, 092004 (1999).
[3] A.W. Thomas, Phys. Lett. **126B**, 97 (1983).
[4] For a recent review see J. Speth and A.W. Thomas, Adv. Nucl. Phys. **24**, 83 (1998); S. Kumano, Phys. Rep. **303**, 183 (1998).
[5] E.M. Henley and G.A. Miller, Phys. Lett. B **251**, 453 (1990); V.R. Zoller, Z. Phys. C **53**, 443 (1992); A. Szczurek and J. Speth, Nucl. Phys. **A555**, 249 (1993); A. Szczurek and H. Holtmann, Acta Phys. Pol. B **24**, 1833 (1993); A. Szczurek, J. Speth, and G.T. Garvey, Nucl. Phys. **A570**, 765 (1994).
[6] S. Paiva *et al.*, Mod. Phys. Lett. A **13**, 2715 (1998).
[7] H. Holtmann, A. Szczurek, and J. Speth, Nucl. Phys. **A569**, 631 (1996).
[8] W. Koepf, L.L. Frankfurt, and M. Strikman, Phys. Rev. D **53**, 2586 (1996).
[9] M. Przybycien, A. Szczurek, and G. Ingelman, Z. Phys. C **74**, 509 (1997).
[10] W. Melnitchouk, J. Speth, and A.W. Thomas, Phys. Rev. D **59**, 014033 (1999).
[11] N.N. Nikolaev, W. Schaefer, A. Szczurek, and J. Speth, Phys. Rev. D **60**, 014004 (1999).
[12] U. D'Alesio, H.J. Pirner, and A. Schaefer, ''Target fragmentation in pp and γp collisions at high energies,'' hep-ph/9806321.
[13] F.S. Navarra, M. Nielsen, and S. Paiva, Phys. Rev. D **56**, 3041 (1997).
[14] N.N. Nikolaev, J. Speth, and B.G. Zakharov, ''Absorptive corrections to the one pion exchange and measurability of the small x pion structure function at HERA,'' hep-ph/9708290.
[15] D.S. Barton *et al.*, Phys. Rev. D **27**, 2580 (1983).
[16] A.E. Brenner *et al.*, Phys. Rev. D **26**, 1497 (1982).
[17] B. Holzenkamp, K. Holinde, and J. Speth, Nucl. Phys. **A500**, 485 (1989).
[18] S. Kumano, Phys. Rev. D **43**, 59 (1991).
[19] Th.A. Rijken, Ann. Phys. (N.Y.) **208**, 253 (1991).
[20] G. Janssen, K. Holinde, and J. Speth, Phys. Rev. C **54**, 2218 (1996), and references therein.